Stabilization of Black Perovskite Phase in $FAPbI_3$ and $CsPbI_3$

*Sofia Masi, Andrés F. Gualdrón-Reyes and Iván Mora-Seró**

Institute of Advanced Materials (INAM), Universitat Jaume I (UJI), Avenida de Vicent Sos Baynat, s/n, 12071 Castellón de la Plana, Spain.

* Corresponding Author: sero@uji.es

Abstract

While halide perovskite allows a great versatility, the application on single absorber solar cells restrings significantly the number of available materials. In this context, $CsPbI_3$ and $FAPbI_3$ (FA, formamidinium) present a huge potentiality for the inorganic nature with enhanced stability the former and the narrow bandgap the later. However, for these materials, Cs^+ and FA^+ are too small and too big relatively, to stabilize the perovskite black phase at room temperature, presenting both a yellow phase non-photoactive as the most stable phase. This fact limits dramatically their application and also help to understand the main research lines in halide perovskite photovoltaics field as the quest for the stabilization of $FAPbI_3$. In this perspective, we overview different strategies for the stabilization of the perovskite black phase of these two materials. We evaluate the stability approaches envisioning efficient and stable materials, with a particular focus to the positive and limiting aspects of the low dimensionality and chemi-structural mechanisms exploitation.

After one decade of intensive work in the halide perovskite field, the versatility of ABX_3 formulation has given rise to a plethora of materials and applications. However, the especial requirements for photovoltaic applications in terms of bandgap, low non-radiative recombination, good transport and long term stability, significantly limits the range of materials available. Narrow bandgap limits the choice of the halide X to I^- and the low non-radiative recombination for the moment is limiting B to Pb^{2+}. In this context the choice of A in order to obtain a 3D material with good transport properties is basically restricted to Cs, methylammonium (MA) and formamidinium (FA).[1] Cs and FA halide perovskites (HP) ride the wave to overpass the established methylammonium based perovskite.[2-4] The interest in these cations originates mostly from the inorganic nature with enhanced stability of the former and from the low bandgap of the latter (1.48 eV for $FAPbI_3$ vs 1.73 eV for $CsPbI_3$).[5] Nonetheless, this potentiality could not be fully developed due to the low stability at room temperature of the optically active perovskite black phase of these materials. The photoactive cubic α-phase quickly transforms into the non-perovskite strain free yellow δ-phase, hexagonal for $FAPbI_3$ or orthorhombic for $CsPbI_3$, resulted from an anisotropic strain in a preferential plane of the α-phase lattice at room temperature.[6]

Iodide perovskites exhibit different optically active polymorphs α- (cubic), β- (tetragonal) and γ- (orthorhombic) black phases, but at room temperature, the δ-yellow phase is the one with the lowest free energy of formation in the case of $CsPbI_3$ and $FAPbI_3$.[7-8] By raising up the temperature, the photoinactive δ-phase can be directly converted in the α-phase, expanding the volume of unit cell. Marronnier *et al.* associated this phase transition to the increase of dynamic motion of $[PbI_6]^{4-}$ octahedra, promoting the connectivity with them.[9] Considering the Goldschmidt tolerance factor (t)[10] and the globularity factor,[1] the energy involved in the process is expected to be higher in order to induce the corner-sharing octahedral geometry when small cations as Cs^+ ($t < 0.8$) are incorporated into the A-site. Conversely, larger cations as FA^+ ($t > 1$) requires lower energies to retain the cubic structure. Thus, the optically active black phase α-$CsPbI_3$ is obtained at T = 300-360 °C,[11] while the α-$FAPbI_3$ is attained at T = 150-185 °C.[12] Although MA^+ cation ($0.8 < t < 1$) as well is demonstrated to favor the formation of an optical black phase (T = 100 °C), $MAPbI_3$ is thermally less stable than pure $FAPbI_3$ or $CsPbI_3$ even under air-absent conditions at T > 85 °C. This fact occurs due to the MA^+ sublimation, and in turn it is not the best candidate in terms of long-term stability.[13]

Even though the black phase of the iodide perovskites is able to prevail after their corresponding synthesis, the unavoidable formation of metastable phases occurs after cooling down process and during their storage, where moisture accelerates the conversion to the yellow phase,[14] that is also influenced by the grain size.[15] The mechanisms involve the hydrolysis of the perovskite and the weak interaction between the cation and the iodide of the inorganic octahedra. The

formamidinium cation with water dissociates in ammonia and sym-triazine,[16] while cesium is intrinsically more stable, being inorganic. In this case the main instability reason lies in its relatively low tolerance factor (<0.8). In both the cases the contraction of the lattice, favoring the interactions between the organic and inorganic moieties, is the current strategy to improve their moisture stability. At low temperature, the applied energy for dynamic motion decreases, breaking the symmetry of cubic structure of connected $[PbI_6]^{4-}$ cages, originated from the octahedral tilting.[17] In this context, the high-symmetry lattice of black phase iodide perovskite is distorted by decreasing the Pb-I-Pb tilting angle (ϕ). For instance, α-$CsPbI_3$ (ϕ = 180 °) converts to β-$CsPbI_3$ (ϕ = 164 °) when T decreases to 265 °C, γ-$CsPbI_3$ (ϕ = 153 °) is reached at 175 °C,[18] while in the case of the $FAPbI_3$ the β- and γ-phases are formed at very low temperature (-122°C and -182°C respectively), see Figure 1.[8]

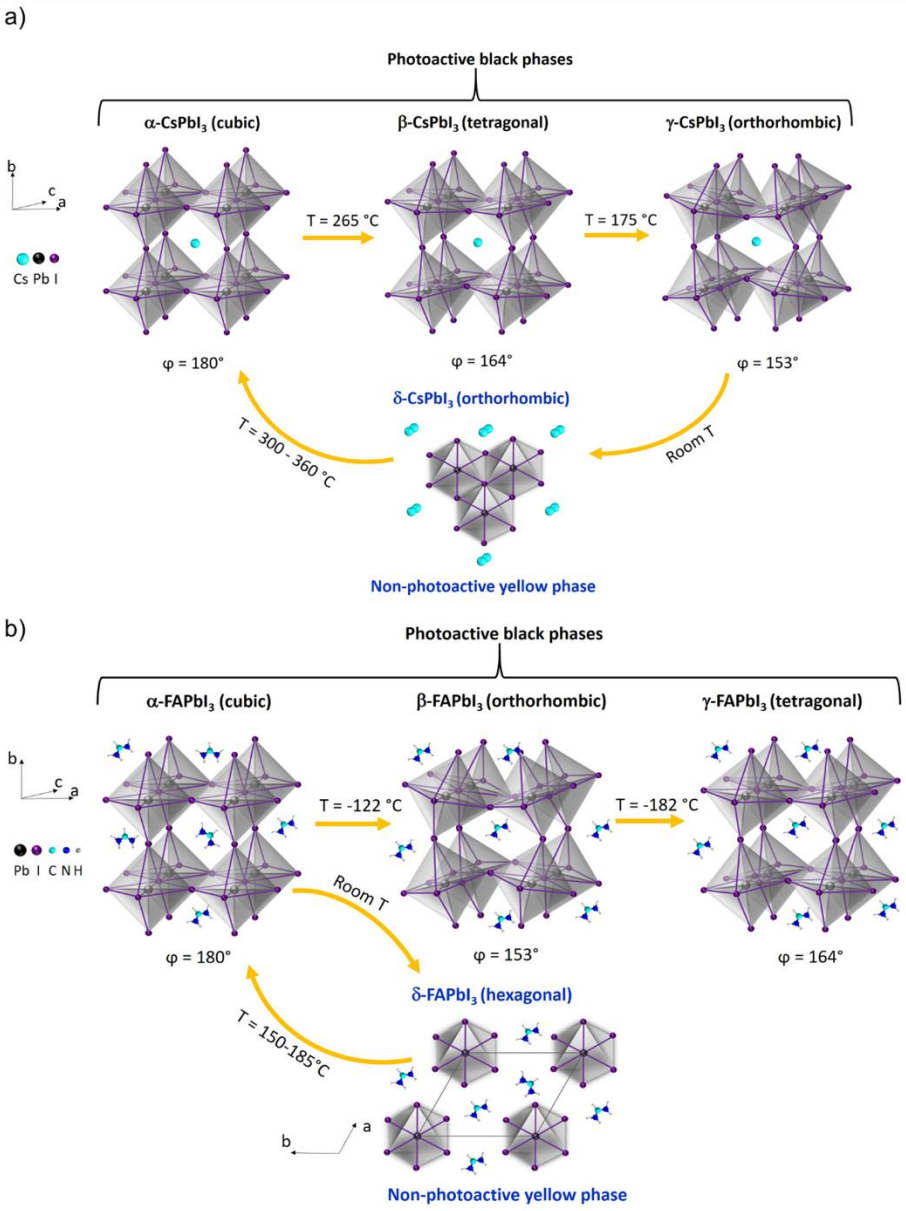

Figure 1. Crystalline structure and polymorphic phase transitions of a) $CsPbI_3$ and b) $FAPbI_3$ perovskites. Non-perovskite δ-yellow phase of both iodide perovskites transforms to black photoactive perovskite α-phase at high temperature. Distortions into the $[PbI_6]^{4-}$ octahedra promote the formation of lowered-symmetric β- and γ-black phases after temperature cools down.

In an ideal active component of an optoelectronic device, long-term ambient degradation cannot be absolutely avoided, as it is inherently coupled with the use in ambient atmosphere, whereas the detrimental thermodynamical stability has no justification and should be minimized. Consequently, for mitigating the black to yellow phase transition of $CsPbI_3$ and $FAPbI_3$ different strategies have been addressed. The literature has reported three main approaches[19]: i) the synthesis

of *low dimensional perovskite materials*, like nanocrystals (NCs). Specifically, the high surface/volume ratio in perovskite NCs (PNCs) is the key factor to attain an enhanced crystalline phase stability compared to their bulk counterpart at room temperature. Thus, the black α-phase in PNCs is stable at room temperature.[20] In this context, the formamidinium based NCs[21-22] are emerging as red emitters, as an alternative to the more consolidated cesium based NCs. ii) *Compositional engineering*, the most extended strategy, where the too small or too big size of Cs^+ and FA^+ cations, respectively, is compensated by the combination of cations and anions of different sizes. Even more components are added in order to obtain black phase stability,[23] where the popular multication/multianion formulation $Cs_{0.05}MA_{0.16}FA_{0.79}Pb(I_{0.83}Br_{0.17})_3$ is a clear model.[24] This strategy has been very effective as since 2014, all the record perovskite solar cells have been attained with multicomponent perovskites,[25] where the FA^+ cation is the main component of the different formulations. However, this approach implies the increase of the perovskite bandgap and the loss of the light harvesting in the NIR region. iii) *The addition of external additives* has been reported to stabilize the α-phase, and to improve the optoelectronic properties. Traditional additives are bulky cations that enables the formation of a 2D/3D perovskite phases, a successful alternative to the 3D perovskite.[26] In some cases the original bandgap could be preserved,[27] and at the same time could passivate defects, leading to improved devices performance.[26] However, additives can also act as cross-linking agents acting at the grain boundaries, reducing the surface energy, like in the case of the bifunctional salt of the ammonium valeric acid iodide (AVAI)[28] or the alkylphosphonic acid ω-ammonium cation.[29] Likewise, sulfobetaine zwitterions are used as chemical stabilizer for the $CsPbI_3$ bulk films, leading to the formation of small and more stable grains.[30] Very recently, the use of PbS QDs is also demonstrated to stabilize the black phase of both the cesium[31] and formamidinium[32] iodide perovskites, due to the similar lattice parameters between the two materials, where the PbS acts as a template, heading the growth of the perovskite where the combination of different chemi-structural effects contributes to the stabilization of the $FAPbI_3$ black phase,[32] as it will be analyzed below.

All these strategies in conclusion evince a control of the lattice strain, correlated with an increase of the vacancy formation energy and in turn with an increase of the stability.[33-34] The enormous interest of $CsPbI_3$ and $FAPbI_3$ and these premises have encouraged still more the synthesis optimization of nanoconfined perovskites in order to take advantage of surface energy and of the strain exploitation to stabilize the perovskite black phase of these materials.[32]

By understanding the correlation between nanocrystal size, lattice strain and energy favorability of the different perovskite phases, critically assessed in this perspective, a development toward stable and optimal bandgap materials is likely to be observed in the imminent future.

Moreover, stable perovskite nanocrystals, allowing for exciton and photon confinement,[35] and stable bulk perovskite, due to its high absorption coefficient,[36] will bring paramount profits either to the photovoltaic (PV)[25] or to the electroluminescent field (EL).[37]

The enormous interest of $CsPbI_3$ and $FAPbI_3$ have encouraged still more the synthesis optimization of nanoconfined perovskites, harnessing surface energy and strain exploitation to stabilize the perovskite black phase.

Perovskite Nanocrystals. PNCs have attracted an enormous interest for optoelectronics, due to their mesmerizing photophysical properties as high photoluminescence quantum yield (PLQY), narrow emission widths and tunable bandgap over the UV-IR spectra, obtained with a relatively easy synthesis processes.[38] Colloidal PNCs with tunable properties can be prepared by harnessing the composition engineering and particle size modulation (quantum confinement effect).[39] Reducing the perovskite size, the contribution of the surface energy (E_{surf}) on the PNC energy formation (Gibbs free energy, E_{PNC}) becomes larger than that of bulk energy (E_{bulk}). This fact decreases the δ-to-α-phase temperature transition.[40] The relationship between E_{PNC}, E_{bulk} and E_{surf} is given for the following equation:[41]

$$E_{PNC} = E_{bulk} + \frac{6E_{surf}V_o}{d} \quad (1)$$

where d is the diameter of PNC, and V_o is the unit cell volume. When PNCs display sizes near to bulk particles, E_{PNC} is dictated by E_{bulk} while E_{surf} is almost negligible.[41-42] However, by increasing the surface area/volume ratio during the formation of PNCs, the number of atoms on the material surface increases and E_{surf} governs E_{PNC}.[43-44]

E_{surf} of α- and γ-$CsPbI_3$, estimated by DFT calculations, are 1.2 and 4.0 meVÅ^{-2}, respectively, while δ-$CsPbI_3$ presents a larger value around 7.5 meVÅ^{-2}. [41] Accordingly, the more negative the E_{surf}, the more negative the E_{PNC}, from which the stabilization of the black phases in $CsPbI_3$ and $FAPbI_3$ PNCs.

Yang et al.[41] have also described the propensity to form α-, γ- and δ-$CsPbI_3$ PNCs in function of the PNC diameter, see Figure 2a. For d values larger than 5.6 nm, δ-$CsPbI_3$ is longer favored, while for d values smaller than 5.6 nm, γ-$CsPbI_3$ is energetically more stable than δ-yellow phase. Further

decreasing d to 3.7 nm, α-$CsPbI_3$ is thermodynamically stabilized and this phase governs the crystalline structure of iodide perovskite with d below 2.7 nm. Therefore, the formation of the α- and γ-phases in the PNCs is thermodynamically more favorable than the inactive δ-phase structure when the PNC size is under nanoscale regime. Conversely, when the PNC size is closer to bulk compounds, the δ-yellow phase is preferred. The limiting aspects of the high surface area/volume ratio is the higher chance to generate surface defects. Despite the defect tolerant structure of the perovskite, proved by the high PLQY,[45] firstly the surface defects act as traps for the photogenerated carriers, compromising the optoelectronic properties, and secondly they contribute to the degradation of the material. To solve this issue, either the healing of the lead iodide octahedra or the control of the chemical equilibria with the surrounding capping ligands are exploited, ultimately improving the stability of the NCs.[46] However, from the point of view of the device application, the long insulating organic chain hinders the charge transport, so a careful control of washing procedure to reduce the ligands but at the same time to preserve the stability is contemplate during the device fabrication. The excess of oleic acid during the NCs preparations allows to reach the certified record PCE of the NCs solar cells of 16.6%, using PNCs $Cs_{0.5}FA_{0.5}PbI_3$.[47] Despite the PCE of pure $CsPbI_3$ NCs based solar cells is lower (14.3%)[48] compared to the 18.4% obtained with the bulk perovskite (Table 1),[49] the use of PNCs instead of the bulk perovskite present some advantages as the enhanced black phase stability, demonstrated for the pure $FAPbI_3$ (Figure 2d, Table 1),[44] or the possibility of creating heterojunctions, exploiting the layer by layer depositions.[50] Thus, the most stable PNCs will be the one where the low dimension is attended with the absence of defects.

The high surface area/volume ratio is also a cause of the compressive strain generation in the perovskite lattice.[20, 51] This effect hampers the octahedral tilting of the material surface, providing more symmetric structures at ambient temperature. Thus, the generation of the non-perovskite δ-yellow phase structure, that requires an expansion in the unit cell volume, is thermodynamically avoided under nanoconfinement, as the energy barrier to promote the phase transformation increases (Figure 2b).[40, 52] Nonetheless, the reversible phase transitions between α-, β- and γ-black phases that occurs into the confined PNCs, due to the slight distortion of the lattice, is less sensitive to the reduction of particle size. These reasons explain the long-time black phase stability of $CsPbI_3$ and $FAPbI_3$ PNCs both in colloidal solution and in thin film,[20, 38, 44] being photoactive for months even under air conditions, see Figure 2c,d. With these evidences, it is clear that a strong spatial confinement (internal, colloidal NC, external, or size restricted by a template) lead to achieve less distorted $CsPbI_3$ structure in films,[53] and more stable PNCs.[31]

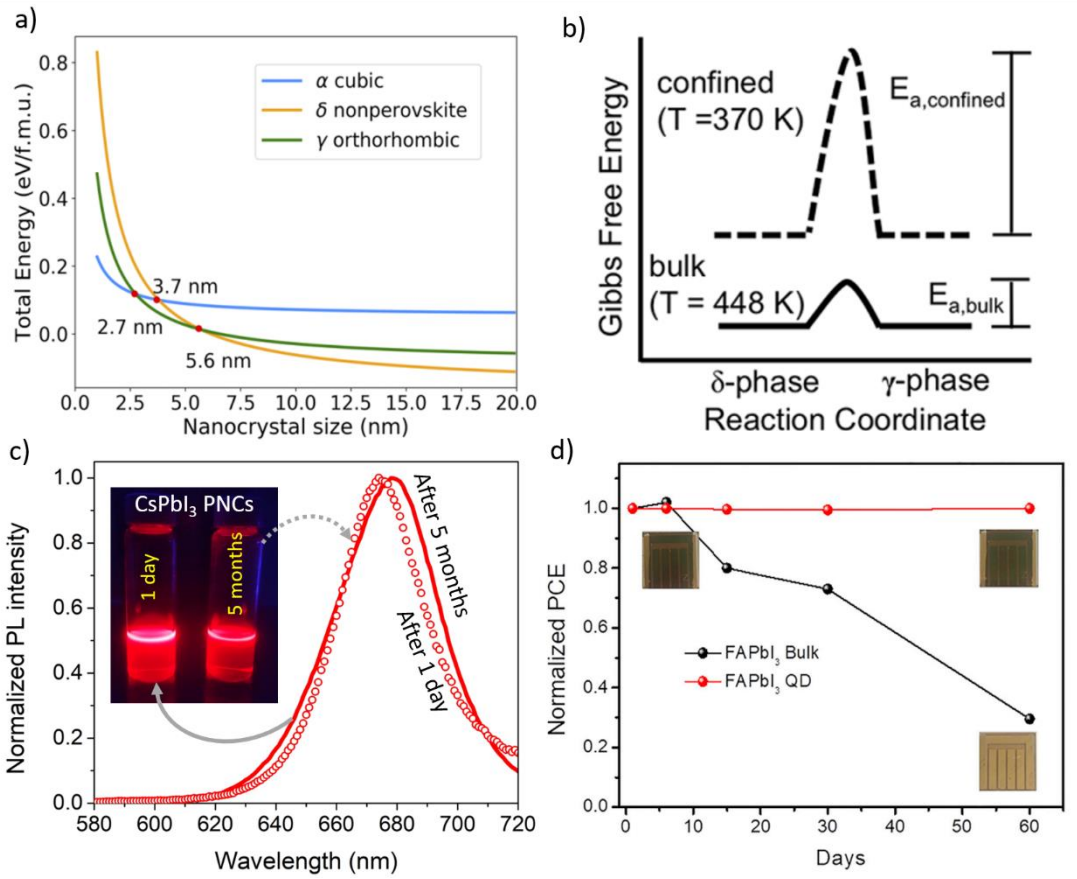

Figure 2. a) Energy formation of the α-, γ- and δ-phases of $CsPbI_3$ PNCs by varying the NC size. Reproduced with permission from ref [41]. Copyright 2020 Royal Chemistry Society. b) Activation energy barrier for the α-to-δ-phase transition for nanoconfined $CsPbI_3$ NCs and bulk crystals. Reproduced with permission from ref.[40]. c) Photoluminescence spectra obtained in our laboratory for $CsPbI_3$ PNCs stored after 1 day and 5 months under air ambient. d) Comparison in the photovoltaic performance of $FAPbI_3$ PNCs and bulk crystals based solar cells after 2 months. Reproduced with permission from ref.[44]. Copyright 2018 Elsevier.

The most stable PNCs will be the one where the low dimension is attended with the absence of defects.

An alternative procedure to lock the formation of the undesired non-photoactive δ-yellow phase in the iodide perovskites is through the use of nanopore templates or scaffolds.[40, 43, 54-56] This approach has been reported to be efficient for confining the perovskite crystal growth by applying physical microstrain, which alters the phase energy free formation. Therefore, the metastable black phases are stabilized at room temperature, keeping their crystal structure even under their decomposition temperature.[40] For instance, Zhao et al. estimated by DFT calculations that γ-$CsPbI_3$ black phase is preferred over δ-$CsPbI_3$ (Figure 3) by extending the surface area greater than 8.6×10^3

m^2 mol^{-1}.[52] On the other hand, Ma *et al.*[43] demonstrated through XRD measurements that the dimensions of the template dictate the strain level to confine the perovskite growth. The microstrain was varied from 1.1 % when $CsPbI_3$ was grown into a 69 nm-pore sized anodized aluminum oxide (AAO) template to 2.0 % by growing the iodide perovskite into a 30 nm-pore sized AAO template. A microstrain value higher than 1.9 % promotes the stabilization of the α-phase. It is worth noting that the application of a minimum compressive strain stabilizes the photoactive black phase even if the surface area of the confined perovskite decreases. By using DFT calculations, the generation of 2.0 % and 2.5 % of microstrain reduce the surface area from the critical value (1.96×10^5 m^2 mol^{-1}) to lower values than 1.82 and 1.75×10^5 m^2 mol^{-1}, respectively, decreasing the phase free energy formation in favor of the α-phase instead of the δ-phase.[43] Definitively, the synthesis of nanoconfined materials is a relevant strategy to be considered during the processing of black-phase iodide perovskites at room temperature, as their intrinsic properties remain basically unchanged.

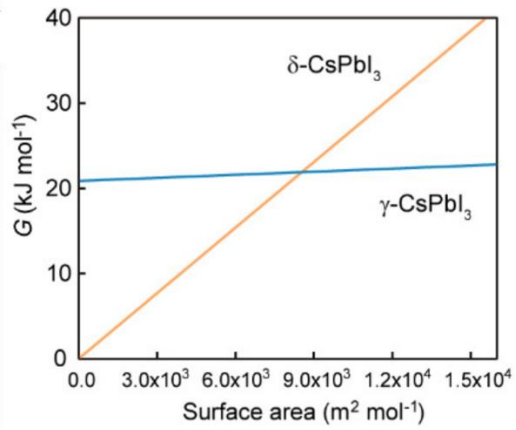

Figure 3. Formation energy dependence, calculated for the γ-$CsPbI_3$ and δ-$CsPbI_3$ phases, in function of the surface area. Reproduced with permission from ref.[52] Copyright 2018 American Chemistry Society.

Compositional engineering. Since its first fabrication report,[57] $FAPbI_3$ showed an enormous potentiality for the development of perovskite solar cells (PSCs), due to its potential higher stability in comparison with $MAPbI_3$ and its narrower bandgap. Black phase $FAPbI_3$ perovskite has in fact the lowest bandgap of the $APbI_3$ family,[58] 1.48 eV, corresponding to a maximal theoretical photoconversion efficiency (PCE_{max}) of 32.3%,[59] and consequently it is *a priori* the most attractive option for single absorber solar cell preparation. However, initial report[57] also highlighted the presence of a yellow polymorph that should be avoided in order to obtain efficient PSCs. Hereafter, most of the compositional work developed in PSCs can be seen as a continuous fight for the stabilization of $FAPbI_3$.

The researchers stabilized $FAPbI_3$ adding smaller cations as MA^+ or Cs^+. In fact, the strategy of mixing FA^+ with other cations have been very successful and the most efficient PSCs have a formamidinium-based perovskite active layer, combined with other cations, such as methylammonium (MA^+),[60] cesium (Cs^+),[61-62] potassium (K^+)[63] or large organic cations forming 2D perovskites.[64-65] For instance, adding certain amounts of Cs^+ cations into the $FAPbI_3$, is a way to obtain a stabilized $FA_{1-x}Cs_xPbI_3$ alloy at room temperature[66] with an increase of the reproducibility if the Rb^+ is also incorporated.[2] As the size of Cs^+ is smaller than the one of FA^+, the tolerance factor is tuned to a suitable region where the black-α-phase cubic structure is attained. The ionic radius of the Cs^+ is smaller than the one of the FA^+, 1.8 Å and 1.9-2.22 Å respectively, thus by mixing FA^+ with MA^+ or Cs^+ the tolerance factor decreases between $0.8 < t < 1$.[67] Based on the same reasoning by mixing the halides like Br^- and Cl^- t is reduced.[68] In this way it is possible to foresee the best combination to obtain a stable black phase. Small cations alone, like the K^+ (ionic radius 1.14 Å) or Rb^+ (ionic radius 1.15 Å) have not adequate dimensions to compensate the stoichiometry reduction of big cations like MA^+ or FA^+, but they are employed in a very effective "cation cascade", to assist in the modification of the crystal lattice of mixed cation/mixed halide perovskite, being responsible for an higher stability to the materials. However a higher amount of Cs^+ or Rb^+ generates a phase segregation, with the formation of $CsPbI_3$ or $RbPbI_3$, due to the large lattice mismatch.[67] Eventually, the mixed cation halide perovskite is transformed into the non-perovskite δ-phase. In the same way a stable α-phase of the mixed halide perovskite,[69] for instance $CsPbBr_{3-x}I_x$, can be reached after adding 33 % Br into perovskite lattice.[38] However, this strategy also has a drawback, as the introduction of MABr salt, produces the blue shift of the $FAPbI_3$ bandgap moving it away from the optimal value in terms of PCE_{max}.[59, 70] For example, the popular multianion/multication $Cs_{0.05}MA_{0.16}FA_{0.79}Pb(I_{0.83}Br_{0.17})_3$ presents a bandgap of 1.63 eV[24] limiting PCE_{max} to 29.8%.[59] Recently, different groups are trying to reduce the perovskite bandgap removing Br^-.[2, 60] This strategy has the current PCE published record of 23.3%[60] with the reduction of bandgap limited to 1.55 eV as 8% of MA^+ has to be added to stabilize the black phase of $FAPbI_3$. The use of Cs^+ instead of MA^+ to stabilize the $FAPbI_3$ perovskite black phase in MA-free $RbCsFAPbI_3$ allows to reduce the bandgap to 1.53 eV.[2] All these results show that the manipulation of perovskite lattice parameters by the addition of alternative cations and anions has the positive effect of the black phase stabilization but unfortunately, in the case of Pb-perovskites, smaller A-site cation produces octahedral tilting resulting in an increased bandgap.[71]

The manipulation of perovskite lattice parameters by the addition of alternative cations and anions produces octahedral tilting resulting in an increased bandgap.

Addition of external additives. The drawback of bandgap blue-shift by the utilization of compositional engineering for the stabilization of perovskite black phase have boost the use of different additives for the stabilization with a minimum impact on the bandgap. Instead of the common MABr salt, a new additive, the methylenediammonium dichloride ($MDACl_2$) is exploited, taking advantage from the more amount of hydrogen bonding that the cation MDA^+ is able to create, and from the well-known stabilizing role of the Cl^-.[3] Along with the $MDACl_2$, the MACl salt is employed as sacrificial additive. The MACl salt degrades during the perovskite formation, leading to a very low amount of extra halide that has a marginal impact on the bandgap of the formamidinium based perovskite. Nevertheless, it has been demonstrated that the low Cl^- amount not only reduces the lattice strain and passivates the interstitial vacancies, but more important has an effective role on the reduction of the lattice parameter of triple halide perovskite,[72] the origin of an increased stability of the α-phase. The role of the MACl salt is also consolidated, as its amount is increased up to 20%[73] and the bandgap of the perovskite is not shifted: the MACl salt is in fact only located at the grain boundaries, acting as external additive for improving the crystallinity of the formamidinium perovskite.

An alternative additive used to stabilize the formamidinium black phase is the above mentioned AVAI,[28] already used for the stabilization of the $MAPbBr_3$ and the $FASnI_3$, confirming the role of the hydrogen bonding in the thermodynamic stabilization, with the novelty that in this case the original bandgap is even slightly red-shifted, allowing to mention it as external additive not incorporated in the crystalline perovskite structure, with no limiting effects on the bandgap.

One strategy in this line is to take benefit from strain. Beyond PNCs, also bulk polycrystalline perovskite films have shown a certain degree of strain, that is reduced when island are formed instead of continuous films.[74] The role of the strain is still under investigation and could be positive or negative towards the perovskite stabilization. Interestingly, most of the literature around the strain focused on materials bearing MA^+,[75] likely because it was the most extensively studied in photovoltaics. Cs^+ is often explored in the case of colloidal nanocrystals,[38] while FA^+ was studied in deep only in the last few years due to its favorable bandgap,[32, 57] whereas the use of other cations such as guanidinium[76-77] is only slightly explored in the field.

As above mentioned, the strain depends on the tilting of the $[PbI_6]^{4-}$ octahedra, easily tuned by the formation of hydrogen bonding between the organic cation and external additives, a very

common approach in the field: the hydrogen bonding determine the orientation of the organic counterpart, that in turn rearrange the tilting of the octahedra.[78] On the other hand, the strain can lead to a faster degradation of the film due to the improved ion migration.[79] This effect occurs when the strain originates from the thermal expansion mismatch of the perovskite lattice parameter with the substrates.[79]

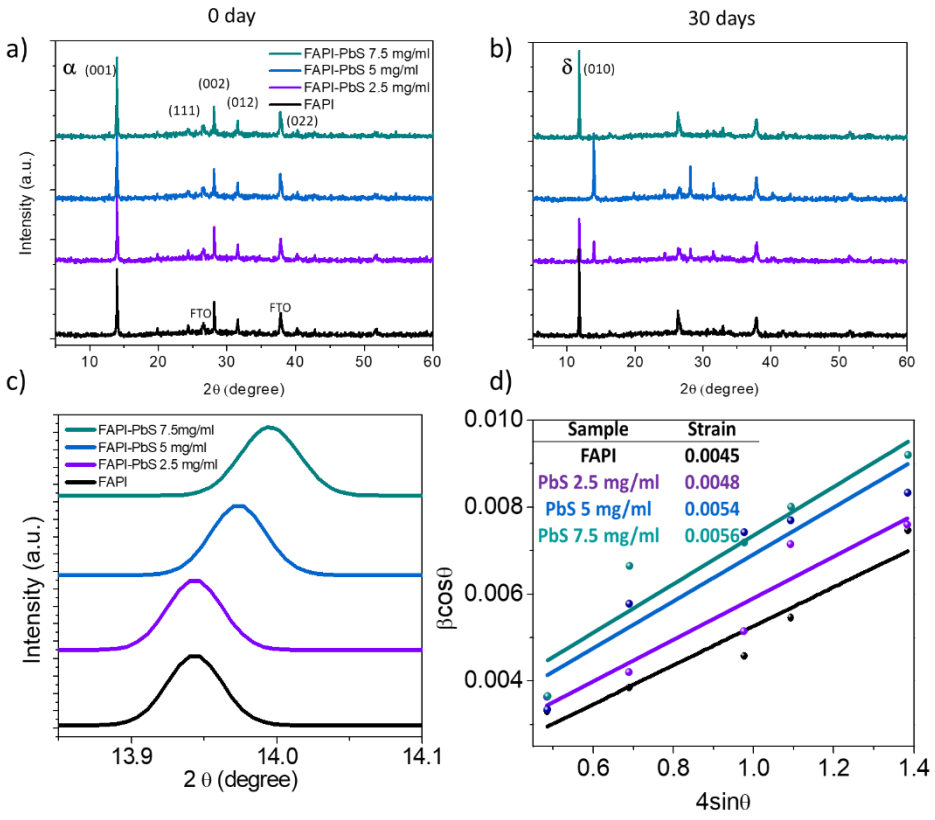

Figure 4. a)-d) Aging test performed on the perovskite thin films without and with 3.8 nm size PbS QDs at different concentrations; XRD patterns of (a) the fresh samples and (b) after 30 days, stored in ambient conditions; d) X-Ray Diffraction pattern of the powders $FAPbI_3$ with and without 8 nm QDs at different concentrations; zoom-in the region around 14°; e) Williamson-Hall fitting: from the slope of the fitting the strain values are obtained; with the permission of ref.[32] Copyright 2020 American Chemistry Society.

However it has been demonstrated that the control of the strain contributes to the stabilization of the α-phase of the formamidinium (Figure 4 e-f) or cesium perovskite film when the PbS QDs are embedded in the $FAPbI_3$ matrix, as a chemical bonding between the PbS and perovskite in the black phase is successfully formed, see Figure 4 e-h.[32] Thus either in the case of the $CsPbI_3$[7] or in the $FAPbI_3$[32] the balanced strain leads to stable materials. The perovskite metastable crystal phase

mimicking the PbS lattice parameters and auto-tuning its tolerance factor, falls down in the stability region and improves the solar cells performances.[31-32] The PbS QDs with lattice parameters close to the one of the perovskite, have been a pioneering choice to demonstrate the positive effect of the strain on the stability, above all if strong chemical bonds between the additive and the desired perovskite phase are created,[32] and alternative rock-salts structure or additives will be in the future to address different circumstances.

Others contributions out of the bare strain have been investigated by Density Functional Theory (DFT) calculation, underlining that only a relatively stabilization is achieved in view of the strain (Figure 5 i). The surface energy created by the interface between $FAPbI_3$ and PbS QDs (Figure 5 ii) and the chemical bonds between both materials (Figure 5 iii) are additional chemi-structural effects in order to stabilize the perovskite black phase (Figure 5 iv).[32]

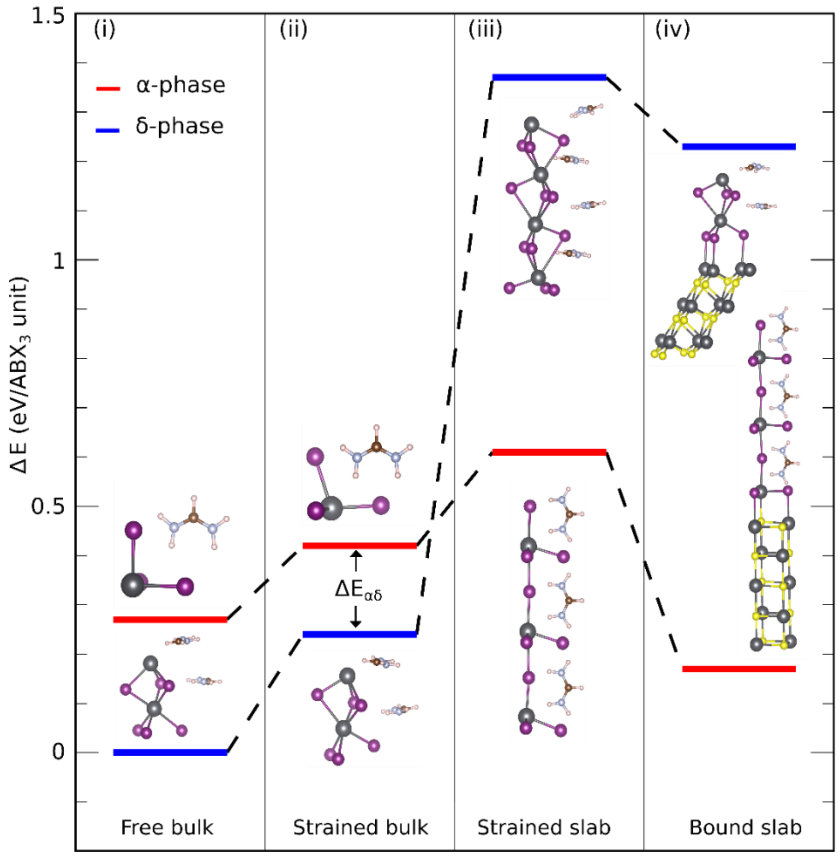

Figure 5. Total energy DFT calculation of (i) black and yellow bulk $FAPbI_3$ phases represented by red and blue colors, respectively, (ii) the effect of strain on the bulk when matching the PbS lattice, (iii) the presence of surfaces in the slabs, and (iv) the role of chemical binding to the PbS substrate in the heterojunctions. The insets

depict the atomic structures under study, which are 3D in (i) and (ii) and 2D in (iii) and (iv). Reproduced with permission from ref.[32] Copyright 2020 American Chemistry Society.

The strain coming from the $FAPbI_3$ accommodation with the lattice parameters of the PbS destabilizes both the black and yellow phases, but the effect is more prominent for the yellow phase; hence the relatively stabilization of the perovskite black phase (Figure 5 ii). In addition, the PbS introduction creates new surface energies, which mostly increase the thermodynamic energy of the yellow phase (Figure 5 iii). Finally the chemical bonds creation between the black phase and the PbS is the main mechanism for the definitive stabilization of the perovskite (Figure 5 iv).

This analysis is a comprehensive picture of the stabilization mechanisms, that paves the way for the investigation also of the chemical interaction between the additive and the yellow phase, that often could be under evaluated, to foresee the best additive for the black phase stabilization along with the destabilization of the photoinactive phase.

All the above mentioned strategies and mechanisms have two parallel consequences, the discussed stabilization of the cesium and formamidinium black perovskite phase and the desired holding of the $FAPbI_3$ bandgap, resulting in turn in stable and high efficiency optoelectronic devices (Figure 6, Table 1). From Figure 6, it is easy to appreciate that longer stabilization times have been reported for $FAPbI_3$ than for $CsPbI_3$, for both bulk and NCs. In the case of photovoltaic devices prepared with bulk black phase $FAPbI_3$ present higher performance than $CsPbI_3$ as it could be expected from the narrower bandgap of the former. Nevertheless, in the case NCs, $CsPbI_3$ NC based solar cells outperform the performance of devices based in $FAPbI_3$ NCs. Indicating that further improvement in the later kind if NCs is required, perhaps because $FAPbI_3$ NCs have been less studied in the literature. However, it should be important to determine if there is an intrinsic limitation in $FAPbI_3$ NCs for further developments.

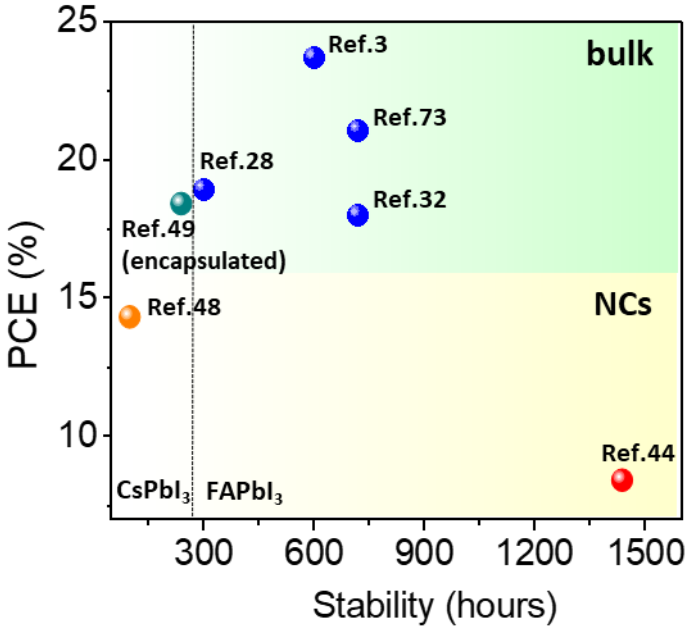

Figure 6. Photoconversion efficiencies (PCE %) against stability (hours); the dots refer to the solar cells fabricated using as active layer the $FAPbI_3$ bulk (blue dots), the $FAPbI_3$ QDs (red dot), the $CsPbI_3$ bulk (cyan dot) and the $CsPbI_3$ QDs (orange dot). In this summary the solar cells obtained with pure perovskite and with perovskite/additives systems which preserve the original bandgap, are reported.

Table 1. Summary of the photoconversion efficiencies (PCE) and stability of the perovskite solar cells based on $FAPbI_3$ and $CsPbI_3$ with external additive, in which the bandgap of the original material is preserved, and based on $CsPbI_3$ NCs. sc-TiO_2: compact TiO_2 layer; m-TiO_2: mesoporous TiO_2 layer; choline iodine (CHI).

Device architecture	PCE (%)	Stability (hours)	Ref.
FTO/c-TiO_2/m-TiO_2/$FAPbI_3$-$MDACl_2$-MACl/passivation layer/Spiro-OMeTAD/Au	23.7	600	(3)
FTO/mTiO_2/c-TiO_2/$FAPbI_3$-AVAI/Spiro-OMeTAD/Au	18.94	300	(28)
FTO/SnO_2/$FAPbI_3$-PbS/Spiro-OMeTAD/Au	18	720	(32)
FTO/SnO_2/$FAPbI_3$-MACl/Spiro-OMeTAD/Ag	21.07	720	(73)
ITO/SnO_2/$FAPbI_3$ NCs/Spiro-OMeTAD/Au	8.38	1440	(44)
FTO/c-TiO_2/CHI-$CsPbI_3$/Spiro-OMeTAD/Ag	18.4	240 (encapsulated)	(49)
FTO/c-TiO_2/s-m-TiO_2/NCs/$CsPbI_3$ NCs/Spiro-OMeTAD/Au	14.3	100	(48)

Furthermore, the compressive strain can lead to a structural compression, which stabilizes the perovskite material. The N-dimethylformamide in acid conditions for the growth of the $MAPbBr_3$,[80] or the PbS QDs for $FAPbI_3$[32] have yield this effect. Consequently, the perovskite emission properties see Figure 7a-d, and the stability in humid conditions[80] are improved. However each time a compressive and unidirectional strain favors the formation of stable perovskite a tensile strain be in

the perpendicular direction, pushing the perovskite in a state of non-equilibrium.[81-82] This phenomenon also could potentially limit the obtainment of an efficient and stable optoelectronic devices;[83] however, because recent research has focused on this topic, we expect that such a limitation could be surpassed with forthcoming strain engineering. In this frame, the chemi-structural mechanisms, taking into account strain but also interfaces and chemical bonds among different materials, will be the future way to stabilize the perovskite desired photoactive phases, or to develop the formation of new phases.[82]

The chemi-structural mechanisms will be the future way to stabilize the perovskite desired photoactive phases, or to develop the formation of new phases.

Another limitation deals with how the strain affects the local recombination,[84] sometimes a challenging analysis due to the heterogeneity of the perovskite structure, that induced mistake in the interpretation of the optoelectronic data collected. An example of these controversies, regards the generation of defects, is the PL quenching observed on $CsPbI_3$,[31] despite previous investigation reported reduced detrimental impact of the PbS QDs in $MAPbI_3$ matrix, or even a beneficial one.[85] In the same way, the PL increases in compressed crystals of $MAPbBr_3$,[80] but not in the microdomains of the $MAPbI_3$ polycrystalline film,[84] see Figure 7e-i. Reasonably the radiative deactivation depends on the specific kind of defects present at the boundary, with its particular chemi-structural surrounding. As the $FAPbI_3$ needs implements to improve the stability, strain and different chemical interactions concerns cannot be eluded.[32] Then the homogeneous propagation of the interactions, as demonstrated by embedding the PbS QDs in the perovskite matrix, is highly desired. In this contest, one of the consequence of the epitaxial growth, taking place from the bulk, like in the case of PbS QDs additives and not from an external substrates, could be the non-radiative recombination reduction in the whole bulk structure.

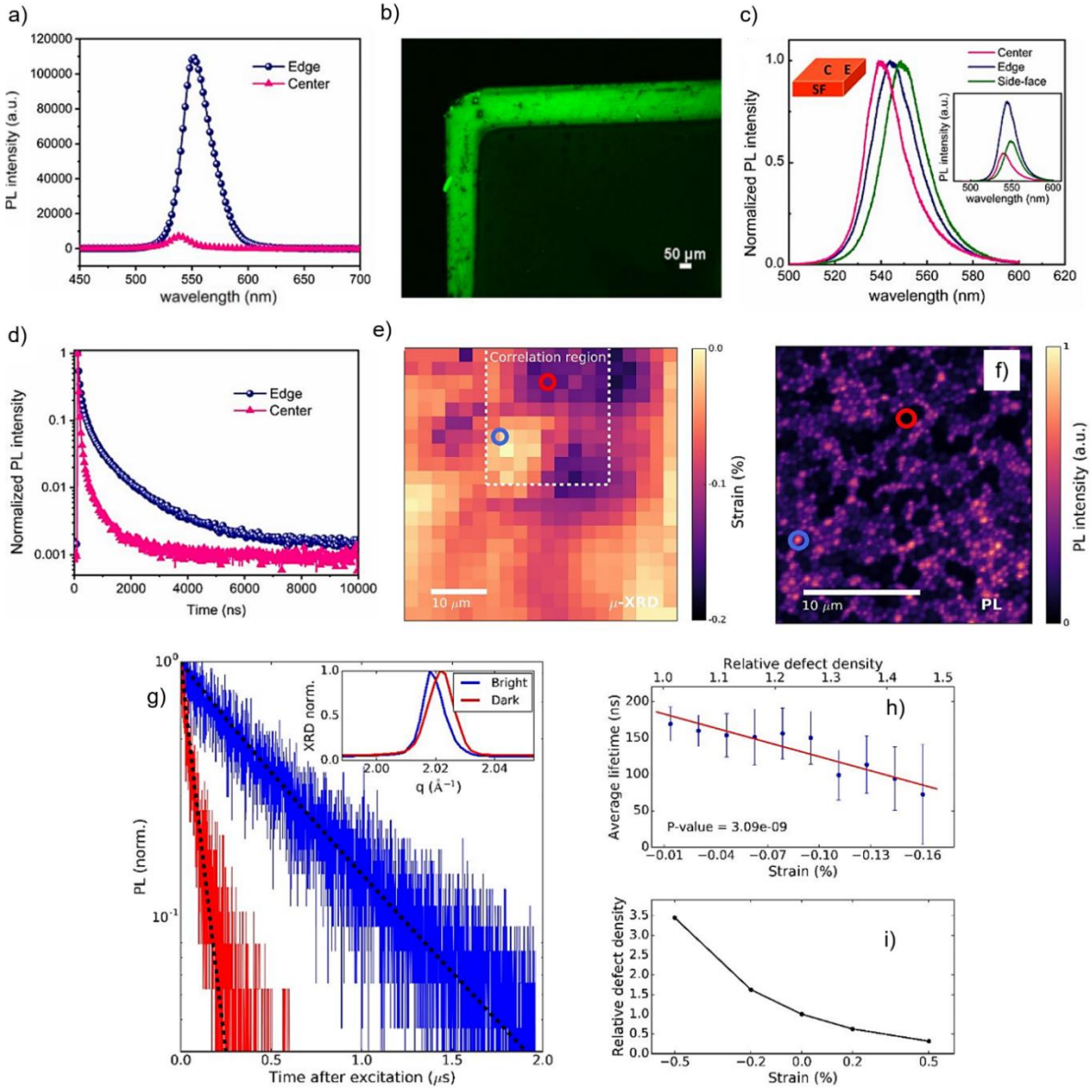

Figure 7. a) Photoluminescence spectrum of the $MAPbBr_3$ single crystal at the edge and center excited at 405 nm. b) Fluorescence confocal images of edge emissive $MAPbBr_3$ single crystal. c) Representative normalized μ-PL emission spectra collected at room temperature under 457 nm laser excitation in different regions of the $MAPbBr_3$ single crystal. Inset: μ-PL spectra without normalization (the sketch in the inset represents the measurement position). d) Normalized PL decay traces of the $MAPbBr_3$ single crystal at the edge and center, excited at 405 nm and collected at the PL emission peak of 552 and 538 nm with 1 nm bandwidth, respectively with the permission of Ref.[80] Copyright 2020 American Chemistry Society.; (e-i) Correlating the local structural and time-resolved luminescence properties of $MAPbI_3$ films. (e) Spatial map of the (compressive) strain variation using the relative shift of the peak q-value at each local point from the minimum q in a μXRD map (i.e. strain = (qmin − q)/qmin). (f) Confocal PL intensity map of a $MAPbI_3$ perovskite film corresponding to the dashed region in a. (g) Time-resolved PL decays of the bright (blue) and dark (red) regions highlighted in (e). (h) Scatter plots of statistically-significant correlations between local PL lifetime and compressive strain

(relative defect density; calculated from relationship in i). (i) Ratio in concentration of charged iodide vacancies (V+I defects) in 〈110〉 strained perovskite crystals to an unstrained crystal; with the permission of ref. [84] Copyright Royal Chemical Society.

The low dimensionality and the control of the chemi-structural properties could offer the potentiality to stabilize perovskite black phase.

Conclusion remarks. Finally, to achieve the thermodynamic stability remains the real challenge for the photoactive perovskite materials. The black phase perovskite stability needs to be finely mastered for achieving stable crystal structure with controlled defects, as a first step to the further development of reproducible and stable devices based on $CsPbI_3$ and $FAPbI_3$. Among the different methods, the exploitation of the low dimensionality (NCs or 2D/3D perovskite), the use of external additives (PbS colloidal QDs) and the use of specific ions (Cl^- or the Rb^+) in mixed cation/halide perovskite, represent the most emerging and significant strategies. Therefore it is expects that in perspective, the combination of these aspects finally will lead to an improvement in materials and devices stability. In detail, the low dimensionality and the control of the chemi-structural environment could offer the potentiality to obtain high stable material without blue-shift of the material bandgap. Chemi-structural mechanisms involving, strain, surface energy and/or chemical bonds need to be carefully controlled in order to revert the natural tendency of these materials to crystallize in the yellow phase at room temperature. It has been in fact reported that by the control of these mechanisms the stability of black phase can be improved, showing how the approaches discussed in this perspective are an effective solution for phase stabilization. From the experimental results reported employing different stabilization methods of the perovskite black phase, longer stabilization has been reported for $FAPbI_3$ than for $CsPbI_3$. Dedicated research will surely allow in the next years important progresses in the field, focusing on the stabilization of these significant materials with the corresponding implications in the development of photovoltaic and optoelectronic devices.

References

1. Gholipour, S.; Ali, A. M.; Correa-Baena, J.-P.; Turren-Cruz, S.-H.; Tajabadi, F.; Tress, W.; Taghavinia, N.; Grätzel, M.; Abate, A.; De Angelis, F.; Gaggioli, C. A.; Mosconi, E.; Hagfeldt, A.; Saliba, M., Globularity-Selected Large Molecules for a New Generation of Multication Perovskites. *Advanced Materials* **2017,** *29* (38), 1702005.

2. Turren-Cruz, S.-H.; Hagfeldt, A.; Saliba, M., Methylammonium-free, high-performance, and stable perovskite solar cells on a planar architecture. *Science* **2018,** *362* (6413), 449-453.
3. Min, H.; Kim, M.; Lee, S.-U.; Kim, H.; Kim, G.; Choi, K.; Lee, J. H.; Seok, S. I., Efficient, stable solar cells by using inherent bandgap of α-phase formamidinium lead iodide. *Science* **2019,** *366* (6466), 749-753.
4. Gao, X.-X.; Luo, W.; Zhang, Y.; Hu, R.; Zhang, B.; Züttel, A.; Feng, Y.; Nazeeruddin, M. K., Stable and High-Efficiency Methylammonium-Free Perovskite Solar Cells. *Advanced Materials* **2020,** *32* (9), 1905502.
5. Eperon, G. E.; Stranks, S. D.; Menelaou, C.; Johnston, M. B.; Herz, L. M.; Snaith, H. J., Formamidinium lead trihalide: a broadly tunable perovskite for efficient planar heterojunction solar cells. *Energy & Environmental Science* **2014,** *7* (3), 982-988.
6. Zheng, X.; Wu, C.; Jha, S. K.; Li, Z.; Zhu, K.; Priya, S., Improved Phase Stability of Formamidinium Lead Triiodide Perovskite by Strain Relaxation. *ACS Energy Letters* **2016,** *1* (5), 1014-1020.
7. Steele, J. A.; Jin, H.; Dovgaliuk, I.; Berger, R. F.; Braeckevelt, T.; Yuan, H.; Martin, C.; Solano, E.; Lejaeghere, K.; Rogge, S. M. J.; Notebaert, C.; Vandezande, W.; Janssen, K. P. F.; Goderis, B.; Debroye, E.; Wang, Y.-K.; Dong, Y.; Ma, D.; Saidaminov, M.; Tan, H.; Lu, Z.; Dyadkin, V.; Chernyshov, D.; Van Speybroeck, V.; Sargent, E. H.; Hofkens, J.; Roeffaers, M. B. J., Thermal unequilibrium of strained black CsPbI₃ thin films. *Science* **2019,** *365* (6454), 679-684.
8. Fabini, D. H.; Stoumpos, C. C.; Laurita, G.; Kaltzoglou, A.; Kontos, A. G.; Falaras, P.; Kanatzidis, M. G.; Seshadri, R., Reentrant Structural and Optical Properties and Large Positive Thermal Expansion in Perovskite Formamidinium Lead Iodide. *Angewandte Chemie International Edition* **2016,** *55* (49), 15392-15396.
9. Marronnier, A.; Roma, G.; Boyer-Richard, S.; Pedesseau, L.; Jancu, J.-M.; Bonnassieux, Y.; Katan, C.; Stoumpos, C. C.; Kanatzidis, M. G.; Even, J., Anharmonicity and Disorder in the Black Phases of Cesium Lead Iodide Used for Stable Inorganic Perovskite Solar Cells. *ACS Nano* **2018,** *12* (4), 3477-3486.
10. Bartel, C. J.; Sutton, C.; Goldsmith, B. R.; Ouyang, R.; Musgrave, C. B.; Ghiringhelli, L. M.; Scheffler, M., New tolerance factor to predict the stability of perovskite oxides and halides. *Science Advances* **2019,** *5* (2), eaav0693.
11. Eperon, G. E.; Paternò, G. M.; Sutton, R. J.; Zampetti, A.; Haghighirad, A. A.; Cacialli, F.; Snaith, H. J., Inorganic caesium lead iodide perovskite solar cells. *Journal of Materials Chemistry A* **2015,** *3* (39), 19688-19695.
12. Zhang, Y.; Kim, S.-G.; Lee, D.-K.; Park, N.-G., CH3NH3PbI3 and HC(NH2)2PbI3 Powders Synthesized from Low-Grade PbI2: Single Precursor for High-Efficiency Perovskite Solar Cells. *ChemSusChem* **2018,** *11* (11), 1813-1823.
13. Dualeh, A.; Gao, P.; Seok, S. I.; Nazeeruddin, M. K.; Grätzel, M., Thermal Behavior of Methylammonium Lead-Trihalide Perovskite Photovoltaic Light Harvesters. *Chemistry of Materials* **2014,** *26* (21), 6160-6164.
14. Ding, X.; Cai, M.; Liu, X.; Ding, Y.; Liu, X.; Wu, Y.; Hayat, T.; Alsaedi, A.; Dai, S., Enhancing the Phase Stability of Inorganic α-CsPbI3 by the Bication-Conjugated Organic Molecule for Efficient Perovskite Solar Cells. *ACS Applied Materials & Interfaces* **2019,** *11* (41), 37720-37725.
15. Yadavalli, S. K.; Zhou, Y.; Padture, N. P., Exceptional Grain Growth in Formamidinium Lead Iodide Perovskite Thin Films Induced by the δ-to-α Phase Transformation. *ACS Energy Letters* **2018,** *3* (1), 63-64.
16. Lee, J.-W.; Kim, D.-H.; Kim, H.-S.; Seo, S.-W.; Cho, S. M.; Park, N.-G., Formamidinium and Cesium Hybridization for Photo- and Moisture-Stable Perovskite Solar Cell. *Advanced Energy Materials* **2015,** *5* (20), 1501310.

17. Bechtel, J. S.; Van der Ven, A., Octahedral tilting instabilities in inorganic halide perovskites. *Physical Review Materials* **2018,** *2* (2), 025401.
18. Stoumpos, C. C.; Kanatzidis, M. G., The Renaissance of Halide Perovskites and Their Evolution as Emerging Semiconductors. *Accounts of Chemical Research* **2015,** *48* (10), 2791-2802.
19. Dunfield, S. P.; Bliss, L.; Zhang, F.; Luther, J. M.; Zhu, K.; van Hest, M. F. A. M.; Reese, M. O.; Berry, J. J., From Defects to Degradation: A Mechanistic Understanding of Degradation in Perovskite Solar Cell Devices and Modules. *Advanced Energy Materials n/a* (n/a), 1904054.
20. Swarnkar, A.; Marshall, A. R.; Sanehira, E. M.; Chernomordik, B. D.; Moore, D. T.; Christians, J. A.; Chakrabarti, T.; Luther, J. M., Quantum dot–induced phase stabilization of α-CsPbI₃ perovskite for high-efficiency photovoltaics. *Science* **2016,** *354* (6308), 92-95.
21. Protesescu, L.; Yakunin, S.; Kumar, S.; Bär, J.; Bertolotti, F.; Masciocchi, N.; Guagliardi, A.; Grotevent, M.; Shorubalko, I.; Bodnarchuk, M. I.; Shih, C.-J.; Kovalenko, M. V., Dismantling the "Red Wall" of Colloidal Perovskites: Highly Luminescent Formamidinium and Formamidinium–Cesium Lead Iodide Nanocrystals. *ACS Nano* **2017,** *11* (3), 3119-3134.
22. Zhang, T.; Li, H.; Yang, P.; Wei, J.; Wang, F.; Shen, H.; Li, D.; Li, F., Room-temperature synthesized formamidinium lead halide perovskite quantum dots with bright luminescence and color-tunability for efficient light emitting. *Organic Electronics* **2019,** *68*, 76-84.
23. Saliba, M., Polyelemental, Multicomponent Perovskite Semiconductor Libraries through Combinatorial Screening. *Advanced Energy Materials* **2019,** *9* (25), 1803754.
24. Saliba, M.; Matsui, T.; Seo, J.-Y.; Domanski, K.; Correa-Baena, J.-P.; Nazeeruddin, M. K.; Zakeeruddin, S. M.; Tress, W.; Abate, A.; Hagfeldt, A.; Grätzel, M., Cesium-containing triple cation perovskite solar cells: improved stability, reproducibility and high efficiency. *Energy & Environmental Science* **2016,** *9* (6), 1989-1997.
25. https://www.nrel.gov/pv/assets/pdfs/best-research-cell-efficiencies.20200406.pdf.
26. Grancini, G.; Nazeeruddin, M. K., Dimensional tailoring of hybrid perovskites for photovoltaics. *Nature Reviews Materials* **2019,** *4* (1), 4-22.
27. Rodríguez-Romero, J.; Sanchez-Diaz, J.; Echeverría-Arrondo, C.; Masi, S.; Esparza, D.; Barea, E. M.; Mora-Seró, I., Widening the 2D/3D Perovskite Family for Efficient and Thermal-Resistant Solar Cells by the Use of Secondary Ammonium Cations. *ACS Energy Letters* **2020**, 1013-1021.
28. Alanazi, A. Q.; Kubicki, D. J.; Prochowicz, D.; Alharbi, E. A.; Bouduban, M. E. F.; Jahanbakhshi, F.; Mladenović, M.; Milić, J. V.; Giordano, F.; Ren, D.; Alyamani, A. Y.; Albrithen, H.; Albadri, A.; Alotaibi, M. H.; Moser, J.-E.; Zakeeruddin, S. M.; Rothlisberger, U.; Emsley, L.; Grätzel, M., Atomic-Level Microstructure of Efficient Formamidinium-Based Perovskite Solar Cells Stabilized by 5-Ammonium Valeric Acid Iodide Revealed by Multinuclear and Two-Dimensional Solid-State NMR. *Journal of the American Chemical Society* **2019,** *141* (44), 17659-17669.
29. Li, X.; Ibrahim Dar, M.; Yi, C.; Luo, J.; Tschumi, M.; Zakeeruddin, S. M.; Nazeeruddin, M. K.; Han, H.; Grätzel, M., Improved performance and stability of perovskite solar cells by crystal crosslinking with alkylphosphonic acid ω-ammonium chlorides. *Nature Chemistry* **2015,** *7* (9), 703-711.
30. Wang, Q.; Zheng, X.; Deng, Y.; Zhao, J.; Chen, Z.; Huang, J., Stabilizing the α-Phase of CsPbI3 Perovskite by Sulfobetaine Zwitterions in One-Step Spin-Coating Films. *Joule* **2017,** *1* (2), 371-382.
31. Liu, M.; Chen, Y.; Tan, C.-S.; Quintero-Bermudez, R.; Proppe, A. H.; Munir, R.; Tan, H.; Voznyy, O.; Scheffel, B.; Walters, G.; Kam, A. P. T.; Sun, B.; Choi, M.-J.; Hoogland, S.; Amassian, A.; Kelley, S. O.; García de Arquer, F. P.; Sargent, E. H., Lattice anchoring stabilizes solution-processed semiconductors. *Nature* **2019,** *570* (7759), 96-101.
32. Masi, S.; Echeverría-Arrondo, C.; Salim, K. M. M.; Ngo, T. T.; Mendez, P. F.; López-Fraguas, E.; Macias-Pinilla, D. F.; Planelles, J.; Climente, J. I.; Mora-Seró, I., Chemi-Structural Stabilization of

Formamidinium Lead Iodide Perovskite by Using Embedded Quantum Dots. *ACS Energy Letters* **2020,** *5* (2), 418-427.
33. Fafarman, A. T., More stable when relaxed. *Nature Energy* **2018,** *3* (8), 617-618.
34. Fu, Q.; Tang, X.; Huang, B.; Hu, T.; Tan, L.; Chen, L.; Chen, Y., Recent Progress on the Long-Term Stability of Perovskite Solar Cells. *Advanced Science* **2018,** *5* (5), 1700387.
35. Shirasaki, Y.; Supran, G. J.; Bawendi, M. G.; Bulović, V., Emergence of colloidal quantum-dot light-emitting technologies. *Nature Photonics* **2013,** *7* (1), 13-23.
36. Park, N.-G., Perovskite solar cells: an emerging photovoltaic technology. *Materials Today* **2015,** *18* (2), 65-72.
37. Chiba, T.; Hayashi, Y.; Ebe, H.; Hoshi, K.; Sato, J.; Sato, S.; Pu, Y.-J.; Ohisa, S.; Kido, J., Anion-exchange red perovskite quantum dots with ammonium iodine salts for highly efficient light-emitting devices. *Nature Photonics* **2018,** *12* (11), 681-687.
38. Protesescu, L.; Yakunin, S.; Bodnarchuk, M. I.; Krieg, F.; Caputo, R.; Hendon, C. H.; Yang, R. X.; Walsh, A.; Kovalenko, M. V., Nanocrystals of Cesium Lead Halide Perovskites (CsPbX3, X = Cl, Br, and I): Novel Optoelectronic Materials Showing Bright Emission with Wide Color Gamut. *Nano Letters* **2015,** *15* (6), 3692-3696.
39. Gualdrón-Reyes, A. F.; Rodríguez-Pereira, J.; Amado-González, E.; Rueda-P, J.; Ospina, R.; Masi, S.; Yoon, S. J.; Tirado, J.; Jaramillo, F.; Agouram, S.; Muñoz-Sanjosé, V.; Giménez, S.; Mora-Seró, I., Unravelling the Photocatalytic Behavior of All-Inorganic Mixed Halide Perovskites: The Role of Surface Chemical States. *ACS Applied Materials & Interfaces* **2020,** *12* (1), 914-924.
40. Kong, X.; Shayan, K.; Hua, S.; Strauf, S.; Lee, S. S., Complete Suppression of Detrimental Polymorph Transitions in All-Inorganic Perovskites via Nanoconfinement. *ACS Applied Energy Materials* **2019,** *2* (4), 2948-2955.
41. Yang, R. X.; Tan, L. Z., Understanding size dependence of phase stability and band gap in CsPbI3 perovskite nanocrystals. *The Journal of Chemical Physics* **2020,** *152* (3), 034702.
42. Zhou, Y.; Zhao, Y., Chemical stability and instability of inorganic halide perovskites. *Energy & Environmental Science* **2019,** *12* (5), 1495-1511.
43. Ma, S.; Kim, S. H.; Jeong, B.; Kwon, H.-C.; Yun, S.-C.; Jang, G.; Yang, H.; Park, C.; Lee, D.; Moon, J., Strain-Mediated Phase Stabilization: A New Strategy for Ultrastable α-CsPbI3 Perovskite by Nanoconfined Growth. *Small* **2019,** *15* (21), 1900219.
44. Xue, J.; Lee, J.-W.; Dai, Z.; Wang, R.; Nuryyeva, S.; Liao, M. E.; Chang, S.-Y.; Meng, L.; Meng, D.; Sun, P.; Lin, O.; Goorsky, M. S.; Yang, Y., Surface Ligand Management for Stable FAPbI3 Perovskite Quantum Dot Solar Cells. *Joule* **2018,** *2* (9), 1866-1878.
45. Liu, F.; Zhang, Y.; Ding, C.; Kobayashi, S.; Izuishi, T.; Nakazawa, N.; Toyoda, T.; Ohta, T.; Hayase, S.; Minemoto, T.; Yoshino, K.; Dai, S.; Shen, Q., Highly Luminescent Phase-Stable CsPbI3 Perovskite Quantum Dots Achieving Near 100% Absolute Photoluminescence Quantum Yield. *ACS Nano* **2017,** *11* (10), 10373-10383.
46. Bodnarchuk, M. I.; Boehme, S. C.; ten Brinck, S.; Bernasconi, C.; Shynkarenko, Y.; Krieg, F.; Widmer, R.; Aeschlimann, B.; Günther, D.; Kovalenko, M. V.; Infante, I., Rationalizing and Controlling the Surface Structure and Electronic Passivation of Cesium Lead Halide Nanocrystals. *ACS Energy Letters* **2019,** *4* (1), 63-74.
47. Hao, M.; Bai, Y.; Zeiske, S.; Ren, L.; Liu, J.; Yuan, Y.; Zarrabi, N.; Cheng, N.; Ghasemi, M.; Chen, P.; Lyu, M.; He, D.; Yun, J.-H.; Du, Y.; Wang, Y.; Ding, S.; Armin, A.; Meredith, P.; Liu, G.; Cheng, H.-M.; Wang, L., Ligand-assisted cation-exchange engineering for high-efficiency colloidal Cs1−xFAxPbI3 quantum dot solar cells with reduced phase segregation. *Nature Energy* **2020,** *5* (1), 79-88.
48. Chen, K.; Jin, W.; Zhang, Y.; Yang, T.; Reiss, P.; Zhong, Q.; Bach, U.; Li, Q.; Wang, Y.; Zhang, H.; Bao, Q.; Liu, Y., High Efficiency Mesoscopic Solar Cells Using CsPbI3 Perovskite Quantum Dots

Enabled by Chemical Interface Engineering. *Journal of the American Chemical Society* **2020,** *142* (8), 3775-3783.
49. Wang, Y.; Dar, M. I.; Ono, L. K.; Zhang, T.; Kan, M.; Li, Y.; Zhang, L.; Wang, X.; Yang, Y.; Gao, X.; Qi, Y.; Grätzel, M.; Zhao, Y., Thermodynamically stabilized β-CsPbI₃–based perovskite solar cells with efficiencies >18%. *Science* **2019,** *365* (6453), 591-595.
50. Li, F.; Zhou, S.; Yuan, J.; Qin, C.; Yang, Y.; Shi, J.; Ling, X.; Li, Y.; Ma, W., Perovskite Quantum Dot Solar Cells with 15.6% Efficiency and Improved Stability Enabled by an α-CsPbI3/FAPbI3 Bilayer Structure. *ACS Energy Letters* **2019,** *4* (11), 2571-2578.
51. Zhao, Q.; Hazarika, A.; Schelhas, L. T.; Liu, J.; Gaulding, E. A.; Li, G.; Zhang, M.; Toney, M. F.; Sercel, P. C.; Luther, J. M., Size-Dependent Lattice Structure and Confinement Properties in CsPbI3 Perovskite Nanocrystals: Negative Surface Energy for Stabilization. *ACS Energy Letters* **2020,** *5* (1), 238-247.
52. Zhao, B.; Jin, S.-F.; Huang, S.; Liu, N.; Ma, J.-Y.; Xue, D.-J.; Han, Q.; Ding, J.; Ge, Q.-Q.; Feng, Y.; Hu, J.-S., Thermodynamically Stable Orthorhombic γ-CsPbI3 Thin Films for High-Performance Photovoltaics. *Journal of the American Chemical Society* **2018,** *140* (37), 11716-11725.
53. Liang, Y.; Huang, X.; Huang, Y.; Wang, X.; Li, F.; Wang, Y.; Tian, F.; Liu, B.; Shen, Z. X.; Cui, T., New Metallic Ordered Phase of Perovskite CsPbI3 under Pressure. *Advanced Science* **2019,** *6* (14), 1900399.
54. Fan, Y.; Meng, H.; Wang, L.; Pang, S., Review of Stability Enhancement for Formamidinium-Based Perovskites. *Solar RRL* **2019,** *3* (9), 1900215.
55. Gu, L.; Zhang, D.; Kam, M.; Zhang, Q.; Poddar, S.; Fu, Y.; Mo, X.; Fan, Z., Significantly improved black phase stability of FAPbI3 nanowires via spatially confined vapor phase growth in nanoporous templates. *Nanoscale* **2018,** *10* (32), 15164-15172.
56. Waleed, A.; Tavakoli, M. M.; Gu, L.; Hussain, S.; Zhang, D.; Poddar, S.; Wang, Z.; Zhang, R.; Fan, Z., All Inorganic Cesium Lead Iodide Perovskite Nanowires with Stabilized Cubic Phase at Room Temperature and Nanowire Array-Based Photodetectors. *Nano Letters* **2017,** *17* (8), 4951-4957.
57. Koh, T. M.; Fu, K.; Fang, Y.; Chen, S.; Sum, T. C.; Mathews, N.; Mhaisalkar, S. G.; Boix, P. P.; Baikie, T., Formamidinium-Containing Metal-Halide: An Alternative Material for Near-IR Absorption Perovskite Solar Cells. *The Journal of Physical Chemistry C* **2014,** *118* (30), 16458-16462.
58. Amat, A.; Mosconi, E.; Ronca, E.; Quarti, C.; Umari, P.; Nazeeruddin, M. K.; Grätzel, M.; De Angelis, F., Cation-Induced Band-Gap Tuning in Organohalide Perovskites: Interplay of Spin–Orbit Coupling and Octahedra Tilting. *Nano Letters* **2014,** *14* (6), 3608-3616.
59. Rühle, S., Tabulated values of the Shockley–Queisser limit for single junction solar cells. *Solar Energy* **2016,** *130*, 139-147.
60. Jiang, Q.; Zhao, Y.; Zhang, X.; Yang, X.; Chen, Y.; Chu, Z.; Ye, Q.; Li, X.; Yin, Z.; You, J., Surface passivation of perovskite film for efficient solar cells. *Nature Photonics* **2019,** *13* (7), 460-466.
61. McMeekin, D. P.; Sadoughi, G.; Rehman, W.; Eperon, G. E.; Saliba, M.; Hörantner, M. T.; Haghighirad, A.; Sakai, N.; Korte, L.; Rech, B.; Johnston, M. B.; Herz, L. M.; Snaith, H. J., A mixed-cation lead mixed-halide perovskite absorber for tandem solar cells. *Science* **2016,** *351* (6269), 151-155.
62. Que, M.; Dai, Z.; Yang, H.; Zhu, H.; Zong, Y.; Que, W.; Padture, N. P.; Zhou, Y.; Chen, O., Quantum-Dot-Induced Cesium-Rich Surface Imparts Enhanced Stability to Formamidinium Lead Iodide Perovskite Solar Cells. *ACS Energy Letters* **2019**, 1970-1975.
63. Yao, D.; Zhang, C.; Pham, N. D.; Zhang, Y.; Tiong, V. T.; Du, A.; Shen, Q.; Wilson, G. J.; Wang, H., Hindered Formation of Photoinactive δ-FAPbI3 Phase and Hysteresis-Free Mixed-Cation Planar Heterojunction Perovskite Solar Cells with Enhanced Efficiency via Potassium Incorporation. *The Journal of Physical Chemistry Letters* **2018,** *9* (8), 2113-2120.

64. Lee, J.-W.; Dai, Z.; Han, T.-H.; Choi, C.; Chang, S.-Y.; Lee, S.-J.; De Marco, N.; Zhao, H.; Sun, P.; Huang, Y.; Yang, Y., 2D perovskite stabilized phase-pure formamidinium perovskite solar cells. *Nature Communications* **2018,** *9* (1), 3021.
65. Niu, T.; Lu, J.; Tang, M.-C.; Barrit, D.; Smilgies, D.-M.; Yang, Z.; Li, J.; Fan, Y.; Luo, T.; McCulloch, I.; Amassian, A.; Liu, S.; Zhao, K., High performance ambient-air-stable FAPbI3 perovskite solar cells with molecule-passivated Ruddlesden–Popper/3D heterostructured film. *Energy & Environmental Science* **2018,** *11* (12), 3358-3366.
66. Li, Z.; Yang, M.; Park, J.-S.; Wei, S.-H.; Berry, J. J.; Zhu, K., Stabilizing Perovskite Structures by Tuning Tolerance Factor: Formation of Formamidinium and Cesium Lead Iodide Solid-State Alloys. *Chemistry of Materials* **2016,** *28* (1), 284-292.
67. Saliba, M.; Matsui, T.; Domanski, K.; Seo, J.-Y.; Ummadisingu, A.; Zakeeruddin, S. M.; Correa-Baena, J.-P.; Tress, W. R.; Abate, A.; Hagfeldt, A.; Grätzel, M., Incorporation of rubidium cations into perovskite solar cells improves photovoltaic performance. *Science* **2016,** *354* (6309), 206-209.
68. Chen, Q.; De Marco, N.; Yang, Y.; Song, T.-B.; Chen, C.-C.; Zhao, H.; Hong, Z.; Zhou, H., Under the spotlight: The organic–inorganic hybrid halide perovskite for optoelectronic applications. *Nano Today* **2015,** *10* (3), 355-396.
69. Dastidar, S.; Egger, D. A.; Tan, L. Z.; Cromer, S. B.; Dillon, A. D.; Liu, S.; Kronik, L.; Rappe, A. M.; Fafarman, A. T., High Chloride Doping Levels Stabilize the Perovskite Phase of Cesium Lead Iodide. *Nano Letters* **2016,** *16* (6), 3563-3570.
70. Shockley, W.; Queisser, H. J., Detailed Balance Limit of Efficiency of p-n Junction Solar Cells. *Journal of Applied Physics* **1961,** *32* (3), 510-519.
71. Prasanna, R.; Gold-Parker, A.; Leijtens, T.; Conings, B.; Babayigit, A.; Boyen, H.-G.; Toney, M. F.; McGehee, M. D., Band Gap Tuning via Lattice Contraction and Octahedral Tilting in Perovskite Materials for Photovoltaics. *Journal of the American Chemical Society* **2017,** *139* (32), 11117-11124.
72. Xu, J.; Boyd, C. C.; Yu, Z. J.; Palmstrom, A. F.; Witter, D. J.; Larson, B. W.; France, R. M.; Werner, J.; Harvey, S. P.; Wolf, E. J.; Weigand, W.; Manzoor, S.; van Hest, M. F. A. M.; Berry, J. J.; Luther, J. M.; Holman, Z. C.; McGehee, M. D., Triple-halide wide–band gap perovskites with suppressed phase segregation for efficient tandems. *Science* **2020,** *367* (6482), 1097-1104.
73. Zhang, Y.; Seo, S.; Lim, S. Y.; Kim, Y.; Kim, S.-G.; Lee, D.-K.; Lee, S.-H.; Shin, H.; Cheong, H.; Park, N.-G., Achieving Reproducible and High-Efficiency (>21%) Perovskite Solar Cells with a Presynthesized FAPbI3 Powder. *ACS Energy Letters* **2020,** *5* (2), 360-366.
74. Chuliá-Jordán, R.; Fernández-Delgado, N.; Juárez-Pérez, E. J.; Mora-Seró, I.; Herrera, M.; Molina, S. I.; Martínez-Pastor, J. P., Inhibition of light emission from the metastable tetragonal phase at low temperatures in island-like films of lead iodide perovskites. *Nanoscale* **2019,** *11* (46), 22378-22386.
75. Wang, J. T.-W.; Wang, Z.; Pathak, S.; Zhang, W.; deQuilettes, D. W.; Wisnivesky-Rocca-Rivarola, F.; Huang, J.; Nayak, P. K.; Patel, J. B.; Mohd Yusof, H. A.; Vaynzof, Y.; Zhu, R.; Ramirez, I.; Zhang, J.; Ducati, C.; Grovenor, C.; Johnston, M. B.; Ginger, D. S.; Nicholas, R. J.; Snaith, H. J., Efficient perovskite solar cells by metal ion doping. *Energy & Environmental Science* **2016,** *9* (9), 2892-2901.
76. Jodlowski, A. D.; Roldán-Carmona, C.; Grancini, G.; Salado, M.; Ralaiarisoa, M.; Ahmad, S.; Koch, N.; Camacho, L.; de Miguel, G.; Nazeeruddin, M. K., Large guanidinium cation mixed with methylammonium in lead iodide perovskites for 19% efficient solar cells. *Nature Energy* **2017,** *2* (12), 972-979.
77. Sánchez, S.; Jerónimo-Rendon, J.; Saliba, M.; Hagfeldt, A., Highly efficient and rapid manufactured perovskite solar cells via Flash InfraRed Annealing. *Materials Today* **2019**.
78. Masi, S.; Aiello, F.; Listorti, A.; Balzano, F.; Altamura, D.; Giannini, C.; Caliandro, R.; Uccello-Barretta, G.; Rizzo, A.; Colella, S., Connecting the solution chemistry of PbI2 and MAI: a cyclodextrin-

based supramolecular approach to the formation of hybrid halide perovskites. *Chemical Science* **2018,** *9* (12), 3200-3208.
79. Zhao, J.; Deng, Y.; Wei, H.; Zheng, X.; Yu, Z.; Shao, Y.; Shield, J. E.; Huang, J., Strained hybrid perovskite thin films and their impact on the intrinsic stability of perovskite solar cells. *Science Advances* **2017,** *3* (11), eaao5616.
80. Boopathi, K. M.; Martín-García, B.; Ray, A.; Pina, J. M.; Marras, S.; Saidaminov, M. I.; Bonaccorso, F.; Di Stasio, F.; Sargent, E. H.; Manna, L.; Abdelhady, A. L., Permanent Lattice Compression of Lead-Halide Perovskite for Persistently Enhanced Optoelectronic Properties. *ACS Energy Letters* **2020,** *5* (2), 642-649.
81. Rolston, N.; Bush, K. A.; Printz, A. D.; Gold-Parker, A.; Ding, Y.; Toney, M. F.; McGehee, M. D.; Dauskardt, R. H., Engineering Stress in Perovskite Solar Cells to Improve Stability. *Advanced Energy Materials* **2018,** *8* (29), 1802139.
82. Zhu, C.; Niu, X.; Fu, Y.; Li, N.; Hu, C.; Chen, Y.; He, X.; Na, G.; Liu, P.; Zai, H.; Ge, Y.; Lu, Y.; Ke, X.; Bai, Y.; Yang, S.; Chen, P.; Li, Y.; Sui, M.; Zhang, L.; Zhou, H.; Chen, Q., Strain engineering in perovskite solar cells and its impacts on carrier dynamics. *Nature Communications* **2019,** *10* (1), 815.
83. Khenkin, M. V.; Katz, E. A.; Abate, A.; Bardizza, G.; Berry, J. J.; Brabec, C.; Brunetti, F.; Bulović, V.; Burlingame, Q.; Di Carlo, A.; Cheacharoen, R.; Cheng, Y.-B.; Colsmann, A.; Cros, S.; Domanski, K.; Dusza, M.; Fell, C. J.; Forrest, S. R.; Galagan, Y.; Di Girolamo, D.; Grätzel, M.; Hagfeldt, A.; von Hauff, E.; Hoppe, H.; Kettle, J.; Köbler, H.; Leite, M. S.; Liu, S.; Loo, Y.-L.; Luther, J. M.; Ma, C.-Q.; Madsen, M.; Manceau, M.; Matheron, M.; McGehee, M.; Meitzner, R.; Nazeeruddin, M. K.; Nogueira, A. F.; Odabaşı, Ç.; Osherov, A.; Park, N.-G.; Reese, M. O.; De Rossi, F.; Saliba, M.; Schubert, U. S.; Snaith, H. J.; Stranks, S. D.; Tress, W.; Troshin, P. A.; Turkovic, V.; Veenstra, S.; Visoly-Fisher, I.; Walsh, A.; Watson, T.; Xie, H.; Yıldırım, R.; Zakeeruddin, S. M.; Zhu, K.; Lira-Cantu, M., Consensus statement for stability assessment and reporting for perovskite photovoltaics based on ISOS procedures. *Nature Energy* **2020,** *5* (1), 35-49.
84. Jones, T. W.; Osherov, A.; Alsari, M.; Sponseller, M.; Duck, B. C.; Jung, Y.-K.; Settens, C.; Niroui, F.; Brenes, R.; Stan, C. V.; Li, Y.; Abdi-Jalebi, M.; Tamura, N.; Macdonald, J. E.; Burghammer, M.; Friend, R. H.; Bulović, V.; Walsh, A.; Wilson, G. J.; Lilliu, S.; Stranks, S. D., Lattice strain causes non-radiative losses in halide perovskites. *Energy & Environmental Science* **2019,** *12* (2), 596-606.
85. Ngo, T. T.; Masi, S.; Mendez, P. F.; Kazes, M.; Oron, D.; Seró, I. M., PbS quantum dots as additives in methylammonium halide perovskite solar cells: the effect of quantum dot capping. *Nanoscale Advances* **2019,** *1* (10), 4109-4118.

AUTHOR INFORMATION

Corresponding Authors

***E-mail:** sero@uji.es (I.M.-S.)

Twitter: @IvanMoraSero (I.M.-S.)

Notes

The authors declare no competing financial interest.

Biographies

Sofia Masi is a postdoc researcher at the Institute of Advanced Materials (INAM) at Universidad Jaume I (Spain). She earned her Ph.D. in Bio-Molecular Nanotechnologies in 2016. Her research topics of interest concern interactions between materials of different nature towards stable optoelectronic devices for renewable energy conversion and emission.

Website: http://www.inam.uji.es/users/sofia-masi

Andrés F. Gualdrón-Reyes is postdoc researcher at Institute of Advanced Materials (INAM) at Universitat Jaume I (Spain). He obtained his Ph.D. in Chemistry at Universidad Industrial de Santander (Colombia) in 2018. Actual research is centered in the photophysical and electronic properties of semiconductor nanocrystals mainly organic/inorganic perovskite quantum dots.

Website: https://scholar.google.com/citations?user=tcadMvYAAAAJ&hl=es

Iván Mora-Seró is Associate Professor at the Institute of Advanced Materials (INAM) at Universidad Jaume I (Spain). His research is focused on crystal growth, nanostructured devices, transport and recombination properties, photocatalysis, electrical characterization of photovoltaic and optoelectronic systems. Recent research activities are focused on new concepts for photovoltaic conversion and LEDs using semiconductor quantum dots and halide perovskites.

Website: http://www.inam.uji.es/research-divisions/research-division-dr-iván-mora-seró

■ ACKNOWLEDGEMENTS

Financial support from the European Research Council (ERC) via Consolidator Grant (724424—No-LIMIT) and Generalitat Valenciana via Prometeo Grant Q-Devices (Prometeo/2018/098) is gratefully acknowledged.

TOC